Eur. Phys. J. B **6**, 473–485 (1998)

THE EUROPEAN PHYSICAL JOURNAL B

Effective interactions and superconductivity in the t-J model in the large-N limit

R. Zeyher[a] and A. Greco[b]

Max-Planck-Institut für Festkörperforschung, Heisenbergstrasse 1, 70569 Stuttgart, Germany

Received: 16 June 1998 / Accepted: 14 July 1998

Abstract. The feasibility of a perturbation expansion for Green's functions of the $t-J$ model directly in terms of X-operators is demonstrated using the Baym-Kadanoff functional method. As an application we derive explicit expressions for the kernel Θ of the linearized equation for the superconducting order parameter in leading order of a $1/N$ expansion. The linearized equation is solved numerically on a square lattice taking instantaneous and retarded contributions into account.
Classifying the order parameter according to irreducible representations $\Gamma_i, i = 1, ... 5$, of the point group C_{4v} of the square lattice and according to even or odd parity in frequency we find that a reasonably strong instability occurs only for even frequency pairing with d-wavelike Γ_3 symmetry. The corresponding transition temperature T_c is $\sim 0.01|t|$ where t is the nearest-neighbor hopping integral. The underlying effective interaction consists of an attractive, instantaneous term and a retarded term due to charge and spin fluctuations. The latter is weakly attractive at low frequencies below $\sim J/2$, strongly repulsive up to $\sim |t|$ and attractive towards even higher energies. T_c increases with decreasing doping δ until a d-wavelike bond-order wave instability is encountered near optimal doping at $\delta_{BO} \sim 0.14$ for $J = 0.3$. T_c is essentially linear in J and rather insensitive to an additional second-nearest neighbor hopping integral t'. A rather striking property of T_c is that it is hardly affected by the soft mode associated with the bond-order wave instability or by the Van Hove singularity in the case with second-nearest neighbor hopping. This unique feature reflects the fact that the solution of the gap equation involves momenta far away from the Fermi surface (due to the instantaneous term) and many frequencies (due to the retarded term) so that singular properties in momentum or frequency are averaged out very effectively.

PACS. 74.20.-z Theories and models of superconducting state – 74.20.Mn Nonconventional mechanisms (spin fluctuations, polarons and bipolarons, resonating valence bond model, anyon mechanism, marginal Fermi liquid, Luttinger liquid, etc.) – 74.72.-h High-T_c compounds

1 Introduction

Many studies of the $t-J$ model suggest that this model is able to describe a large body of the low-energy physics of real high-T_c superconductors [1,2]. This is true for many normal state properties of high-T_c oxides where accurate numerical predictions of the $t-J$ model are available for the comparison with experiment. Whether the phenomenon of high-T_c superconductivity itself can be explained within this model is presently not so clear. There are several calculations yielding instabilities of the normal state with respect to d-wave superconductivity [2–5] and also reasonably high values for the transition temperature T_c [6–9]. These calculations, however, use often somewhat uncontrolled assumptions, making definite conclusions difficult. There is also the view [1] that the large observed values for T_c are not directly related to large mean field T_c's in isolated CuO_2 planes described by the $t-J$ model. Instead it is argued that pair tunneling between planes enhances strongly weak, plane-related superconducting instabilities producing in this way the phenomen of high-T_c superconductivity.

In this paper we present a new attempt to calculate T_c for the $t-J$ model in a well controlled way. Similar as in references [3,4] we do not assume the validity of Migdal's theorem or approximate the self-energy by the lowest skeleton graphs. Instead we assume that $1/N$ can be considered as a small parameter where N is the number of electronic degrees of freedom per site. N consists of two spin directions times $N/2$ copies of the local electronic orbital counted by a flavor index. Similar like in many slave boson calculations [3,4,10] the flavor index is introduced in a somewhat artificial way just to make N a large integer. The $SU(2)$ spin symmetry of the original model is thus enlarged to the symplectic group $Sp(N/2)$. The original constraint of having no double occupancies of sites

[a] e-mail: zeyher@greta5.mpi-stuttgart.mpg.de

[b] *Permanent address*: Departamento de Física, Facultad de Ciencias Exactas e Ingeniería and IFIR(UNR-CONICET), Av. Pellegrini 250, 2000 Rosario, Argentina.

is modified to the condition that at most $N/2$ electrons can occupy the N states at each site. Compared to references [3,4] our treatment exhibits two novel features. First, the constraint is implemented in a different and more rigorous way yielding differences in the equation for the superconducting gap already in the leading order $O(1/N)$. Secondly, we have solved the linearized gap equation numerically obtaining also values for T_c. Our conclusions about the occurrence of superconductivity in the $t-J$ model are thus no longer based only on Fermi surface averaged, static coupling strengths as in references [3,4,10,11].

Regarding constraints their implementation in the X-operator approach is trivial [12]. Mathematically, the constraint means that the sum over diagonal elements of X-operators at a given site has to be equal to $N/2$. This sum commutes with every X-operator and thus is a multiple of the identity operator in any irreducible representation of X-operators. Enforcing the constraint means therefore just to select the correct subspace of Hilberts space where the eigenvalue of this sum is equal to $N/2$. In slave boson theory the X-operators are represented by products of slave operators and the Hilbert space is enlarged to the Hilbert space of slave particles. The constraint means now that at each site the number operator of slave particles has to be equal $N/2$. This condition can obviously not hold as an operator identity, *i.e.*, cannot be enforced at any position of an expectation value of slave operators. However, it should be enforced at all positions which originally separated X-operators. Such an enforcement for a fixed N seems to be in conflict with the Bose condensation of the bosonic slave particles as well as the independence of fermion and bosonic slaves in the limit $N \to \infty$. Using the Dirac method to enforce constraints on the operator level it has indeed been shown [13] that the commutator relations for the slave particles have to be changed and that, for instance, the fermionic and the bosonic slave operators no longer commute with each other. In view of this open problems we use in Sections 2 and 3 a perturbation expansion directly in X-operators following the work of reference [14]. This procedure will give us also the opportunity to compare the $O(1/N)$ expression for the gap equation with that of the slave boson approach to see whether the $1/N$ expansions are really the same in the two cases. The final analytic results for the gap equation have already been presented in reference [9], however, without derivations. These derivations can be found in Sections 2 and 3.

The second new feature of our work deals with the solution of the gap equation. Previous work using $1/N$ expansions concluded from Fermi surface averaged, static coupling constants on the occurrence of superconductivity. Our previous work [9,11] has shown that superconducting instabilities occur for any symmetry channel, doping and both for $J=0$ and $J \neq 0$. The point is more whether the corresponding T_c is very small or large enough to be relevant. T_c here is understood as the transition temperature within mean-field theory. This means that the lowering of T_c due to fluctuations in the superconducting order parameter is not taken into account. This assumption is justified if one compares with real, three-dimensional superconductors but does not apply, of course, to strictly two-dimensional models where fluctuations drive the order parameter to zero at any finite temperature. In order to determine T_c one has to solve the gap equation which has several non-BCS features: the kernel of the linearized gap equation consists of an instantaneous and a retarded term and both are characterized by different cutoffs. Moreover, the presence of the instantaneous term does not allow to restrict the momenta to the Fermi surface. Consequently, we solved the gap equation by numerical means. Our method is also suitable to investigate the question of odd frequency pairing [15] in our model. In this case the instantaneous term drops out but the full frequency dependence of the kernel must be kept in addition to the momentum dependence along the Fermi line. Results for odd frequency pairing will also be presented in Section 4 together with the conclusions.

2 Model and general equations for the electron Green's function

The Hamiltonian of the $t-J$ model can be written as

$$H = \sum_{\substack{ij \\ p=1\ldots N}} \frac{t_{ij}}{N} X_i^{p0} X_j^{0p} + \sum_{\substack{ij \\ p,q=1\ldots N}} \frac{J_{ij}}{4N} X_i^{pq} X_j^{qp} - \sum_{\substack{ij \\ p,q=1\ldots N}} \frac{J_{ij}}{4N} X_i^{pp} X_j^{qq}. \quad (1)$$

Let us consider first the case $N=2$. Assuming one orbital per site and excluding double occupancies of sites there are three states $|_i^p\rangle$ at each atom i. $p=0$ denotes the empty state, and $p=1,2$ singly occupied states with spin up and down. The Hubbard operators X_i^{pq} can be represented as projection operators $X_i^{pq} = |_i^p\rangle\langle_i^q|$ and obey the following commutator and anticommutator relations

$$[X_i^{pq}, X_j^{rs}]_\pm = \delta_{ij}(\delta_{qr} X_i^{ps} \pm \delta_{sp} X_i^{rq}), \quad (2)$$

and the completeness relation

$$\sum_{p=0}^{2} X_i^{pp} = 1. \quad (3)$$

The upper (lower) sign in equation (2) holds for bosonlike or mixed (fermionlike) Hubbard operators defined by $p,q>0$ or $p=q=0$ ($p=0, q>0$ or $p>0, q=0$). For $i=j$ both the upper and lower signs hold in each case. The first term in equation (1) describes the hopping of particles between the sites i and j with matrix elements t_{ij}. The second term in equation (1) denotes the Heisenberg interaction between the spin densities at site i and j with the exchange constants J_{ij}. The third term in equation (1) represents the charge-charge interaction of the $t-J$ model. In the following we consider J_{ij} only between nearest neighbors ($J_{ij}=J$) and t_{ij} between nearest ($t_{ij}=t$)

and next nearest ($t_{ij}=t'$) neighbors. We also use always $|t|$ as energy unit.

The Hamiltonian in equation (1) is a generalization from $N=2$ to an (even) arbitrary integer N. The orbital index p consists now of the spin and a flavor index, the latter enumerating $N/2$ identical orbitals at a site. The symmetry group of H is the symplectic group $Sp(N/2)$. For $N>2$ the operators X can no longer be written as projection operators in some basis. Instead, fermionlike (bosonlike or mixed ones) operators are assumed to satisfy the anticommutator (commutator) relations of equation (2). Only some of the diagonal operators can assumed to retain their projection properties, namely, $(X_i^{pp})^2=X_i^{pp}$ for $p>0$. Most other relations characteristic of projection operators such as $X_i^{10}X_i^{01}=X_i^{11}$ are lost for $N>2$. The completeness relation equation (3) is replaced by the constraint

$$Q_i=\sum_{p=0}^{N}X_i^{pp}=N/2. \tag{4}$$

By explicit construction of the Hilbert space and the action of the $X's$ on its vectors one can show [12] that the above properties, together with H, specify completely the problem. In particular, X_i^{00} is a non-negative operator. As a result, equation (4) means that at most $N/2$ particles can occupy the N available states at a site. In this way one may expect that expectation values of observables approach smoothly the physical case $N=2$ from large $N's$ yielding a basis for $1/N$ expansions. We also would like to point out that slave boson treatments of H have many features in common with our approach. However, the Hilbert spaces are different in the two cases as well as the enforcement of the constraint equation (4). Q_i commutes with all Hubbard operators and thus is proportional to the identiy in any irreducible representation of the X-operators. Enforcement of the constraint means in our case just the selection of the correct subspace of the Hilbert space where equation (4) is satisfied as an operator identity.

Following the Baym-Kadanoff procedure [16–18] we define a non-equilibrium Matsubara Green's function of two fermionic operators $X(1)$ and $X(2)$ by

$$G(12)=-\langle TSX(1)X(2)\rangle/\langle S\rangle, \tag{5}$$

$$S=Te^{\int d1X(1)K(1)}. \tag{6}$$

The number 1 stands for an internal pair index p,q as well as a site and a (imaginary) time index i,τ. $\int d1$ means $\sum_{p,q,i}\int_0^\beta d\tau$, where β is the inverse temperature. In equations (5, 6) T is the time ordering operator and K an external source term which is assumed to couple only to bosonic X-operators. We also introduce the non-equilibirum expectation value of bosonic X-operators by

$$L(1)=\langle TSX(1)\rangle/\langle S\rangle. \tag{7}$$

Using the Hamiltonian equation (1) the Heisenberg equation of motion for fermionic operators becomes

$$\frac{\partial}{\partial\tau_1}X(1)=\int d2d3t(123)X(2)X(3), \tag{8}$$

with

$$t(123)=\delta(\tau_2-\tau_1)\delta(\tau_3-\tau_1)\frac{(t_{i_1i_3}\delta_{i_1i_2}+J_{i_1i_2}/2\delta_{i_1i_3})}{N}\times\Big[\delta_{q_10}\delta_{q_30}(1-\delta_{p_30})(\delta_{p_20}\delta_{q_2q_1}\delta_{p_3p_1}+\delta_{p_2p_1}\delta_{q_2p_3})-\delta_{p_10}\delta_{p_30}(1-\delta_{q_30})(\delta_{p_2q_3}\delta_{q_2q_1}+\delta_{p_2p_1}\delta_{q_20}\delta_{q_3q_1})\Big]. \tag{9}$$

Equation (9) agrees with equation (5) of reference [19] if the different sign convention for the hopping term is taken into account. Using equation (8) and rewriting higher-order correlation functions in terms of functional derivatives with respect to K the equation of motion for G can be written as

$$\int d2(G_0^{-1}(12)-\Sigma'(12))G(21')=Q(11'), \tag{10}$$

$$\Sigma'(12)=-\int d3t(132)L(3)+\int d3d4d5t(134)G(45)\Gamma(52,3), \tag{11}$$

$$\Gamma(12,3)=\delta G^{-1}(12)/\delta K(3). \tag{12}$$

G_0 is the unperturbed Green's function

$$G_0^{-1}(12)=-\delta(1-2)\frac{\partial}{\partial\tau_2}-\delta(\bar1-\bar2)(K^{00}(\bar1)\delta_{q_1q_2}-K^{q_1q_2}(\bar1)). \tag{13}$$

Q is given by

$$Q(11')=\delta(1-1')(L^{pq'}(\bar1)\delta_{qp'}+L^{p'q}(\bar1)\delta_{q'p}), \tag{14}$$

where the index $1=(pq,i,\tau)$ has been split into $1=(pq,\bar1)$ with $\bar1=(i\tau)$. L can be expressed by G so the above system of equations for G, the self-energy Σ', and the vertex Γ is closed.

For our purposes it is more convenient to use a normalized Green's function g which obeys a Dyson equation with the usual δ-function on its right-hand side. Writing

$$g(11')=\int d2G(12)Z^{-1}(21'), \tag{15}$$

and requesting that Z satisfies the following equation

$$Z(11')=Q(11')-\int d3d4d5t(134)g(45)\frac{\delta Z(51')}{\delta K(3)}, \tag{16}$$

equations (10–12) assume the form

$$\int d2(G_0^{-1}(12)-\Sigma(12))g(21')=\delta(1-1'), \tag{17}$$

$$\Sigma(12)=-\int d3t(132)L(3)+\int d3d4d5t(134)g(45)\gamma(52,3), \tag{18}$$

$$\gamma(12,3) = \delta g^{-1}(12)/\delta K(3). \quad (19)$$

From equations (17, 19) follows, moreover, the equation for the vertex

$$\gamma(11',3) = \alpha(11';3) + \int d4d5\Theta(11',45)\gamma(45,3), \quad (20)$$

with

$$\alpha(11',3) = \frac{\delta G_0^{-1}(11')}{\delta K(3)} - \int d4 \frac{\delta \Sigma(11')}{\delta L(4)} \frac{\delta L(4)}{\delta K(3)}, \quad (21)$$

$$\Theta(11',45) = \int d6d7 \frac{\delta \Sigma(11')}{\delta g(67)} g(64)g(57). \quad (22)$$

In equation (22) we have replaced the functional derivative of g with respect to K by the vertex γ using Dyson's equation which also leads to a sign change. The above equations are exact and hold both in the normal and the superconducting state. In the normal state the two internal index pairs in $G(12)$ must obey either $p_1 = q_2 = 0$ or $p_2 = q_1 = 0$. From Dyson's equation follows then that the same holds for $Q(12)$ whereas the possible indices in $G_0(12)$, $\Sigma(12)$, and $g(12)$ obey either $p_1 = p_2 = 0$ or $q_1 = q_2 = 0$. In the superconducting state there are no such restrictions; the only general requirement is that all these indices are associated with fermionic operators.

The self-energy is a functional of g and L, *i.e.*,

$$\Sigma = \Sigma[g, L]. \quad (23)$$

In order to derive the linearized equation for the anomalous self-energy we split Σ into the normal part Σ_N and a small anomalous part Σ_{an}. Expanding equation (23) up to linear terms we obtain

$$\Sigma_{an}(11') = \int d2d3 \Big(\frac{\delta \Sigma(11')}{\delta g(23)}\Big)_N \delta g(23) + \int d2 \Big(\frac{\delta \Sigma(11')}{\delta L(2)}\Big)_N \delta L(2), \quad (24)$$

where δg and δL are of first order in the anomalous part and the subscript N means that the functional derivatives are to be taken in the normal state. Now δL has no linear contribution due to gauge invariance and thus drops out in equation (24). Calculating δg from Dyson's equation (17) in linear approximation we obtain

$$\Sigma_{an}(11') = \int d2d3\Theta(11',23)\Sigma_{an}(23), \quad (25)$$

where Θ is given by equation (22) with all quantities taken in the normal state. Equation (25) represents the linearized equation for a general order parameter for superconductivity. In order to have superconductivity the homogenous equation (25) must have a nonvanishing solution for Σ_{an}. The highest temperature where this occurs is the transition temperature T_c.

The basic quantitity to be calculated is according to equation (25) the kernel Θ. In order to find a functional equation for Θ we get from equation (18)

$$\frac{\delta \Sigma(11')}{\delta g(78)} = \int d2t(127)\gamma(81',2) + \int d2d3d6t(123)g(36)\frac{\delta \gamma(61',2)}{\delta g(78)}, \quad (26)$$

and from equation (20)

$$\frac{\delta \gamma(61',2)}{\delta g(78)} = \frac{\delta \alpha(61',2)}{\delta g(78)} + \int d9'd10'\Theta(61',9'10')\frac{\delta \gamma(9'10',2)}{\delta g(78)} + \int d9'd10' \frac{\delta \Theta(61',9'10')}{\delta g(78)} \gamma(9'10',2). \quad (27)$$

Solving equation (27) for $\delta\gamma/\delta g$, inserting the result into equation (26) and inserting equation (26) into equation (22) yields an exact functional equation for Θ.

3 1/N expansion for the kernel Θ

The equation for Θ obtained in the previous section is too difficult to be solved directly. On the other hand it is exact and holds for any N so it may serve as a starting point for approximate treatments. In the following we assume that $1/N$ may be used as a small parameter and calculate Θ up to order $1/N$. This will allow us to obtain the gap equation (25) in leading order of the $1/N$ expansion.

The N-dependence of an equilibrium quantity is determined by the number of coupling constants it contains and the number of free internal summations. In equilibrium, *i.e.*, without the source term K, we have, for instance,

$$g\begin{pmatrix} 0q_1 & 0q_2 \\ \bar{1} & \bar{2} \end{pmatrix} = \delta_{q_1 q_2} g(\bar{1} - \bar{2}), \quad (28)$$

$$\Sigma\begin{pmatrix} 0q_1 & 0q_2 \\ \bar{1} & \bar{2} \end{pmatrix} = \delta_{q_1 q_2} \Sigma(\bar{1} - \bar{2}), \quad (29)$$

$$\gamma\begin{pmatrix} oq_1 & oq_2 & p_3 q_3 \\ \bar{1} & \bar{2}, & \bar{3} \end{pmatrix} = \frac{-1}{N}\delta_{p_3 q_3}\delta_{q_1 q_2}\gamma_c(\bar{1}\bar{2}, \bar{3}) + \delta_{q_1 p_3}\delta_{q_2 q_3}\gamma_s(\bar{1}\bar{2}, \bar{3}), \quad (30)$$

and similar expressions for α and Θ. In equations (28–30) all the indices $q_1, q_2, ...$ are assumed to be larger than zero. The equilibrium Green's function g, the self-energy Σ, the charge vertex γ_c and the spin vertex γ_s are free of internal indices. In the following we need only the leading $O(1)$ contributions for these quantities. From equations (13, 17, 19) follows that the spin vertex becomes then simply equal to $\delta(\bar{1} - \bar{2})\delta(\bar{1} - \bar{3})$. Using the constraint equation (4) one also recognizes that the charge vertex γ_c defined in equation (30) is equal to the element $q_1 = q_2 > 0, p_3 = q_3 = 0$

of the general vertex γ on the left-hand side of equation (30) which is the motivation to use prefactors in equation (30) in defining γ_c.

Decomposing the labels 1,1′, *etc.* into their internal and external parts the anomalous self-energy or order parameter has the form $\Sigma_{an}\begin{pmatrix} p_1 0 & 0 q_1' \\ \bar{1} & \bar{1}' \end{pmatrix}$, or in more detail, $\Sigma_{an}\begin{pmatrix} \sigma_1 m_1 0 & 0 \sigma_1' m_1' \\ \bar{1} & \bar{1}' \end{pmatrix}$. In the following we are interested in order parameters which are structureless in the flavor indices, *i.e.*, we assume always $m_1 = m_1'$. With respect to spin indices we consider either singlet or triplet pairing. Both cases are included if we put $\sigma_1 = -\sigma_1'$. Correspondingly we will write for the internal indices $p_1, \bar{p}_1$ thus indicating the special relationship between these two indices. Exposing explicitly the internal indices the gap equation (25) becomes

$$\Sigma_{an}\begin{pmatrix} p_1 0 & 0 \bar{p}_1 \\ \bar{1} & \bar{1}' \end{pmatrix} = \sum_{p_2} \int d2d3\Theta \begin{pmatrix} p_1 0 & 0 \bar{p}_1 & p_2 0 & 0 \bar{p}_2 \\ \bar{1} & \bar{1}', & \bar{2} & \bar{3} \end{pmatrix} \Sigma_{an}\begin{pmatrix} p_2 0 & 0 \bar{p}_2 \\ \bar{2} & \bar{3}, \end{pmatrix} \quad (31)$$

where Θ is to be taken in the normal state. Equation (31) also makes visible which indices for Θ are actually needed in the gap equation. A closer examination shows that the first two contributions on the right-hand side of equation (27) are of higher orders in $1/N$ than the third term in this equation for the needed combination of indices. Dropping these terms and inserting equations (26, 27) into equation (22) yields the following equation for Θ valid up to $O(1/N)$ and for the above combinations of internal indices:

$$\begin{aligned} \Theta(11', 910) = &\int d2d7d8t(127)\gamma(81', 2)g(79)g(108) \\ &+ \int d2d3d6d7d8d9'd10't(123)g(36) \\ &\times \frac{\delta\Theta(61', 9'10')}{\delta g(78)}\gamma(9'10', 2)g(79)g(108). \end{aligned} \quad (32)$$

The first term on the right-hand side of equation (32) could have been also obtained directly from equation (18). Conssidering only anomalous contributions to Σ the first term on the right-hand side of equation (18) cannot contribute, wheras the second one can contribute in two ways: a) *via* an anomalous g and a normal vertex γ, b) *via* a normal g and an anomalous vertex γ. Case (a) corresponds to the usual situation of Eliashberg theory and also of the slave boson treatment of superconductivity in the $t-J$ model in $O(1/N)$: Σ_{an} consists then of a Fock diagram containing an anomalous Green's function and an effective interaction taken in the normal state. Linearizing g in Σ_{an} case (a) immediately yields the first term on the right-hand side of equation (32). Its evaluation is straightforward and shows that it is of $O(1/N)$ for the relevant combination of internal indices. This indicates that $T_c \to 0$ for $N \to \infty$ which agrees with the fact that at $N = \infty$ the system consists of renormalized, but non-interacting fermions.

The leading contribution of the second term on the right-hand side of equation (32) is obtained by taking the spin-flip part in the hopping matrix element t and the spin vertex γ_s in $O(1)$ for the vertex γ. As a result only one sum over internal indices survives.The second term in equation (32) is of $O(1/N)$ if the two functions

$$g^{(1)}(\bar{6}\bar{1}', \bar{2}|\bar{7}\bar{8}) = \sum_{p_3} \frac{\delta\Theta\begin{pmatrix} p_3 0 & 0 \bar{p}_1 & 0 p_1 & 0 p_3 \\ \bar{6} & \bar{1}', & \bar{2} & \bar{2} \end{pmatrix}}{\delta g\begin{pmatrix} \bar{p}_1 0 & 0 p_1 \\ \bar{7} & \bar{8} \end{pmatrix}}, \quad (33)$$

$$g^{(2)}(\bar{6}\bar{1}', \bar{2}|\bar{7}\bar{8}) = \sum_{p_3} \frac{\delta\Theta\begin{pmatrix} p_3 0 & 0 \bar{p}_1 & p_3 0 & p_1 0 \\ \bar{6} & \bar{1}', & \bar{2} & \bar{2} \end{pmatrix}}{\delta g\begin{pmatrix} \bar{p}_1 0 & 0 p_1 \\ \bar{7} & \bar{8} \end{pmatrix}}, \quad (34)$$

are of $O(1)$. Equations for $g^{(i)}, i = 1, 2$ can be obtained from equation (32) by taking appropriate derivatives. An examination of the various terms shows that terms with a second functional derivative of Θ are smaller by a factor $1/N$ compared to the leading ones and thus can be neglected. One then finds that the functions $g^{(i)}$ have the form

$$g^{(1)}(\bar{6}\bar{1}', \bar{2}|\bar{7}\bar{8}) = \delta(\bar{2} - \bar{8})g^{(1)}(\bar{6}\bar{1}', \bar{2}|\bar{7}), \quad (35)$$

$$g^{(2)}(\bar{6}\bar{1}', \bar{2}|\bar{7}\bar{8}) = \delta(\bar{2} - \bar{7})g^{(1)}(\bar{6}\bar{1}', \bar{2}|\bar{8}). \quad (36)$$

The reduced functions $g^{(i)}(\bar{6}\bar{1}', \bar{2}|\bar{8})$ (the use of the same name for corresponding functions with different number of arguments should not cause any confusion) satisfy the integral equation

$$\begin{aligned} g^{(i)}(\bar{1}, \bar{1}', \bar{2}|\bar{7}) = &h^{(i)}(\bar{1}, \bar{1}', \bar{2}|\bar{7}) \\ &- \int d\bar{3}d\bar{4}d\bar{6}Nt(\bar{1}\bar{3}\bar{4})g(\bar{6}\bar{4})g^{(i)}(\bar{6}\bar{1}', \bar{3}|\bar{7})g(\bar{2}\bar{3}), \end{aligned} \quad (37)$$

with

$$h^{(1)}(\bar{1}\bar{1}', \bar{2}|\bar{7}) = Nt(\bar{1}\bar{1}'\bar{7})g(\bar{2}\bar{1}'), \quad (38)$$

$$h^{(2)}(\bar{1}\bar{1}', \bar{2}|\bar{7}) = -\int d\bar{3}d\bar{4}Nt(\bar{1}\bar{3}\bar{4})\gamma_c(\bar{7}\bar{1}', \bar{3})g(\bar{4}\bar{2}). \quad (39)$$

Here $t(\bar{1}\bar{2}\bar{3})$ denotes the external part of $t(123)$, *i.e.*, the first three factors outside of the bracket in equation (9). Inserting the explicit expression for t into equation (37) one finds that equation (37) represents an integral equation for $g^{(i)}$ with a kernel consisting of not more than 6 separable contributions. The solution of equation (37) thus reduces to the inversion of at most 6×6 matrices similar as in the case of the charge vertex γ_c dicussed in reference [19].

Inserting the resulting expressions back into equation (32) and performing Fourier transforms one obtains after some elementary, but tedious algebra the following results. The linearized gap equation (25) becomes

$$\Sigma_{an}(k) = -\frac{T}{NN_c}\sum_{k'}\Theta(k,k')\frac{1}{\omega_{n'}^2+\epsilon^2(\mathbf{k}')}\Sigma_{an}(k'). \quad (40)$$

N_c is the number of cells and k the supervector $k=(n,\mathbf{k})$, where n denotes a fermionic Matsubara frequency $\omega_n = (2n+1)\pi T$ with T being the temperature. $\epsilon(\mathbf{k})$ is the one-particle energy with momentum $\mathbf{k}$ in the limit $N\to\infty$ given by the implicit equation

$$\epsilon(\mathbf{k}) = \frac{\delta}{2}t(\mathbf{k}) - J(\mathbf{k})\cdot\frac{1}{N_c}\sum_{\mathbf{p}}\cos(p_x)f(\epsilon(\mathbf{p}-\mu)) \quad (41)$$

where δ is the doping, $t(\mathbf{k})$ and $J(\mathbf{k})$ the Fourier transforms of the coupling constants t_{ij} and J_{ij}, respectively, μ is the chemical potential and f the Fermi function.

The kernel Θ in equation (40) consists of four different terms

$$\Theta(k,k') = \Theta^{(1)}(k,k') + \Theta^{(2)}(k,k') + \Theta^{(3)}(k,k') + \Theta^{(4)}(k,k'). \quad (42)$$

The first two terms are given by

$$\Theta^{(1)}(k,k') = \mp t(\mathbf{k}') \mp J(\mathbf{k}-\mathbf{k}') - t(\mathbf{k}') - J(\mathbf{k}-\mathbf{k}'), \quad (43)$$

$$\Theta^{(2)}(k,k') = (t(\mathbf{k}') + J(\mathbf{k}-\mathbf{k}'))(\gamma_c(k,k'-k)+1). \quad (44)$$

Here, γ_c is the charge vertex in $O(1)$ determined by

$$\gamma_c(k,q) = -1 + \sum_{\alpha,\beta=1}^{6} F_\alpha(k)(1+\chi(q))^{-1}_{\alpha\beta}\chi_{\beta 2}(q), \quad (45)$$

with the susceptibility matrix

$$\chi_{\alpha\beta}(q) = \frac{1}{N_c}\sum_{\mathbf{k}} E_\alpha(\mathbf{k},\mathbf{q})F_\beta(\mathbf{k})\frac{f(\epsilon(\mathbf{k}+\mathbf{q})) - f(\epsilon(\mathbf{k}))}{\epsilon(\mathbf{k}+\mathbf{q}) - \epsilon(\mathbf{k}) - i\nu_n}\cdot \quad (46)$$

q is the supervector $q=(\mathbf{q}, i\nu_n)$ where ν_n denotes the bosonic Matsubara frequency $2\pi nT$. The two vectors E and F are given by

$$E_\alpha(\mathbf{k},\mathbf{q}) = (1, t(\mathbf{k}+\mathbf{q}) + J(\mathbf{q}), \cos k_x, \sin k_x, \cos k_y, \sin k_y), \quad (47)$$

$$F_\beta(\mathbf{k}) = (t(\mathbf{k}), 1, J\cos k_x, J\sin k_x, J\cos k_y, J\sin k_y). \quad (48)$$

The explicit expressions for the third and fourth contributions to Θ are

$$\Theta^{(3)}(k,k') = -\sum_{r=1}^{5}\tilde{E}_r(-\mathbf{k})\tilde{\chi}_{2r}(k-k')\gamma(k,k'-k) + \sum_{r,s=1}^{5}\tilde{E}_s(-\mathbf{k})\tilde{\chi}_{rs}(k-k')\tilde{V}_r(k-k'), \quad (49)$$

$$\Theta^{(4)}(k,k') = \pm\sum_{r,s=1}^{5}(\tilde{E}_s(-\mathbf{k})\tilde{\chi}_{rs}(k+k'))(\tilde{F}_r(-\mathbf{k}') + \tilde{W}_r(k+k')), \quad (50)$$

with the vectors $\tilde{V}$ and $\tilde{W}$

$$\tilde{V}_r(k-k') = \sum_{s=1}^{5}(1+\tilde{\chi}(k-k'))^{-1}_{rs}\tilde{\chi}_{2,s}(k-k')\gamma_c(k,k'-k), \quad (51)$$

$$\tilde{W}_r(k+k') = -\sum_{s,t=1}^{5}(1+\tilde{\chi}(k+k'))^{-1}_{rs}\tilde{F}_t(-\mathbf{k}')\tilde{\chi}_{ts}(k+k'). \quad (52)$$

The vectors $\tilde{E}$ and $\tilde{F}$ have five components and are obtained from the six-component vectors E and F by omitting the second component. In an analogues way, $\tilde{\chi}_{2,s}$ is obtained from the second row of the matrix χ by omitting the second element. Similarly, the 5×5 matrix $\tilde{\chi}$ is obtained from the 6×6 matrix χ by dropping the second row and second column. The upper (lower) signs in the contibutions $\Theta^{(i)}$ refer to singlet (triplet) pairings.

The kernel $\Theta(k,k')$ is invariant under the transformations of the point group C_{4v} of the square lattice. As a result $\Sigma_{an}(k)$ transforms corresponding to one of the five irreducible representations Γ_i of C_{4v}, and it can be chosen to be either even or odd in Matsubara frequencies. Γ_1 corresponds to singlet s- or extended s-wave, Γ_3 to singlet d-wave- and Γ_5 to triplet p-wave pairing for even frequency pairing. The linearized gap equation (40) splits completely into its irreducible parts. This also means that the momenta $\mathbf{k},\mathbf{k}'$ can be restricted to 1/8 of the Brillouin zone which greatly simplifies the numerical solution of equation (40). In the following we will deal with even frequency pairing unless the opposite is explicitly stated and drop for simplicity the index which differentiates between even and odd frequency-pairing. The irreducible kernels and order parameters will thus be denoted by $\Theta_i(k,k')$ and $\Sigma_{an,i}(k)$, respectively.

4 Discussion of the gap equation and numerical results

According to equation (42) the total kernel Θ is the sum of four contributions. The first one, $\Theta^{(1)}$, represents the instantaneous part of Θ. From equation (40) follows that positive values for $\Theta^{(1)}$ correspond to repulsion, negative values to attraction between electrons. Keeping only $\Theta^{(1)}$ and decomposing it into its irreducible symmetry components the gap equation (40) becomes for the representation $i=1...5$ of the point group C_{4v} of a square lattice

$$\Sigma_{i,an}(\mathbf{k}) = \frac{-1}{NN_c}\sum_{\mathbf{k}'}\Theta_i^{(1)}(\mathbf{k},\mathbf{k}')\chi(\mathbf{k}')\Sigma_{i,an}(\mathbf{k}'), \quad (53)$$

with

$$\chi(\mathbf{k}') = \frac{\tanh((\epsilon(\mathbf{k}')-\mu)/T)}{2(\epsilon(\mathbf{k}')-\mu)}, \tag{54}$$

$\Theta_2^{(1)} = \Theta_4^{(1)} = \Theta_5^{(1)} = 0$, and

$$\Theta_1^{(1)}(\mathbf{k},\mathbf{k}') = 8|t|\eta_1(\mathbf{k}') - 8J\eta_1(\mathbf{k})\eta_1(\mathbf{k}'), \tag{55}$$

$$\Theta_3^{(1)}(\mathbf{k},\mathbf{k}') = -8J\eta_3(\mathbf{k})\eta_3(\mathbf{k}'). \tag{56}$$

In equations (55, 56) we assumed nearest-neighbor hopping with $t_{ij} = -|t|$ and used the basis functions $\eta_1(\mathbf{k}) = (\cos(k_x)+\cos(k_y))/2, \eta_3(\mathbf{k}) = (\cos(k_x)-\cos(k_y))/2$. Inserting the kernels equations (55, 56) into the gap equation yields the following conditions for a finite T_c:

$s-$wave pairing ($\Sigma_{an} \sim$ *constant*):

$$1 + a|t| + \frac{ab_1|t|J}{1-Jb_1} = 0, \tag{57}$$

extended $s-$wave pairing ($\Sigma_{an} \sim \eta_1(\mathbf{k})$):

$$1 - b_1 + \frac{ab_1|t|J}{1+a|t|} = 0, \tag{58}$$

$d-$wave pairing ($\Sigma_{an} \sim \eta_3(\mathbf{k})$):$1 - b_3 J = 0.$ (59)

Here we used the following abbreviations

$$a = \frac{8}{NN_c}\sum_{\mathbf{k}'}\chi(\mathbf{k}')\eta_1(\mathbf{k}'), \tag{60}$$

$$b_l = \frac{8}{NN_c}\sum_{\mathbf{k}'}\chi(\mathbf{k}')\eta_l^2(\mathbf{k}'), \tag{61}$$

for $l = 1,\ 3$. A numerical evaluation shows that in the interesting parameter region $0 \le J \le 0.3, 0 \le \delta \le 0.8$ (δ is the doping) and at low temperaturs a, b_1, b_3 are positive and $b_1 < 3$. This means that there is never an instability with respect to constant s-wave pairing. b_1 is an increasing, b_3 a strongly decreasing function with increasing δ and these two functions cross around $\delta \sim 0.6$. Thus d-wave pairing is stable in any case for $\delta < 0.5$. For $0.5 \le \delta \le 0.8$ $a|t|$ is much larger than 1 so that the third term in equation (58) cancels the second term to a large extent making extended s-wave pairing also in this region unfavourable. Thus we find that the instantaneous contribution to the kernel strongly favours d-wave pairing in the interesting parameter regime. The reason for this is to a large extent a band structure effect: b_3 is much larger than b_1 at small dopings because of large contributions around the X-point. At larger doping the competing extended s-wave pairing is strongly suppressed by its coupling to the hopping term, which ultimately is caused by the constraint.

$\Theta^{(2)}$, $\Theta^{(3)}$, and $\Theta^{(4)}$ are retarded contributions to Θ. $\Theta^{(2)}$ is mainly determined by collective charge fluctuations due to the poles of γ_c. $\Theta^{(3)}$ and $\Theta^{(4)}$ originate from the anomalous part of the vertex and involve both charge and spin fluctuations. The latter dominate in $\Theta^{(4)}$ in agreement with the sign change between its singlet and triplet contribution. Quantitatively, $\Theta^{(4)}$ is by far the largest of the retarded contributions. Our Θ does not contain terms which are related to the magnons of the undoped case. Such contributions are of higher order in $1/N$ than those considered above and are thus neglected.

Our expression for Θ is different from that of the slave boson approach [3]. Σ_{an} in the slave boson approach essentially consists of a spinon Fock term with an effective interaction taken in the normal state times an anomalous spinon Green's function. Such an contribution clearly corresponds to the case (a) discussed after equation (32), *i.e.*, to the first term on the right-hand side of equation (32), or, equivalently. to the sum of $\Theta^{(1)}$ and $\Theta^{(2)}$. Our contributions $\Theta^{(3)}$ and $\Theta^{(4)}$ have no analogue in the slave boson approach though they are clearly also of $O(1/N)$. The differences between the two approaches can be made more explicitly by considering two limiting cases. For $J \to 0$ Θ reduces to equation (9) of reference [11] The underlying interactions are still spin-dependent as can be seen from the singlet versus triplet case. Such a dependence on spin is not present in the corresponding slave boson expression [10]. Furthermore, the high-frequency limit of Θ, *i.e.*, $\Theta^{(1)}$ should be identical to that of the slave boson expression if the two approaches are equivalent. The slave boson result for $\Theta^{(1)}$ differs, however, from equation (43): the argument in one of the two hopping terms is replaced by $\mathbf{k}$ and there is an additional term proportional to $1/\delta$. Equation (5) agrees, however, with previous X-operator results based on the diagrammatic methods for X-operators, for instance, equation (35) of reference [20]. The expression for $\Theta^{(1)}$ of reference [7] contains only one of the two hopping terms $t(\mathbf{k}')$ of equation (5) which, we think, is incorrect. The general question then arises why is it possible to obtain different $O(1/N)$ expressions for the same quantitiy in the two approaches using the same Hamiltonian. The differences arise because different Hilbert spaces are used in the two cases. This difference is already indicated in the definition of the order parameters for superconductivity. In the X-operator approach all vectors of the Hilbert space are eigenvectors of the constraints Q_i with eigenvalue $N/2$. Expectation values of operators are only nonzero if, in the slave boson language, the number of created slave particles is equal to the number of annihilated slave particles in these operators. The superconducting order parameter of slave boson theory, on the other hand, consists of the expectation values $\langle b\rangle$ and $\langle c^\dagger c^\dagger\rangle$. Clearly, these expectation values have no analogues in the X-operator approach.

4.1 Eigenvalues of Θ in the static limit

In the weak-coupling case it is often assumed that the solution of the gap equation (40) is of BCS-type for each symmetry Γ_i, *i.e.*,

$$T_{ci} = 1.13\omega_c e^{1/\lambda_i}. \tag{62}$$

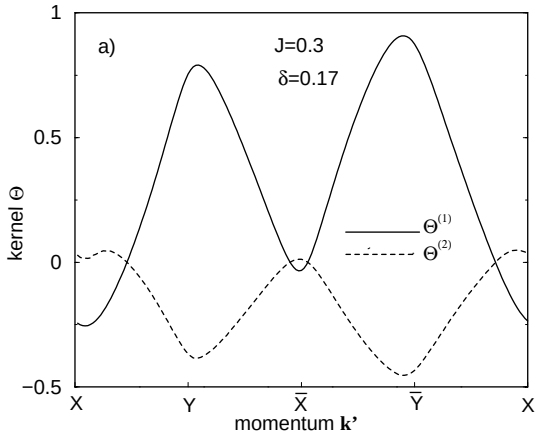

(a)

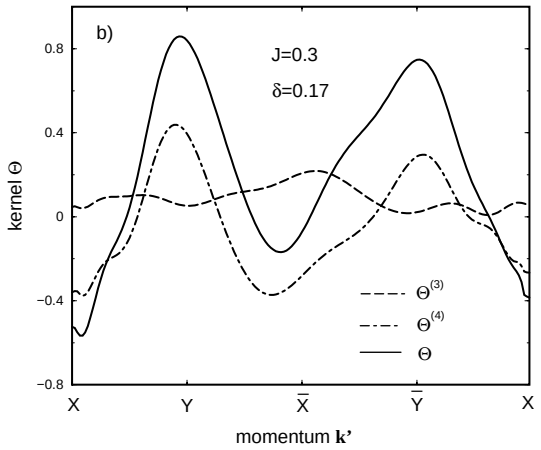

(b)

Fig. 1. Dependence of various contributions to the total kernel Θ on the second momentum $\mathbf{k}'$ along the Fermi line for a fixed first momentum $\mathbf{k} = (2.465, 0.309)$; (a) Contributions $\Theta^{(1)}, \Theta^{(2)}$; (b) Contributions $\Theta^{(3)}, \Theta^{(4)}$, and the total Θ.

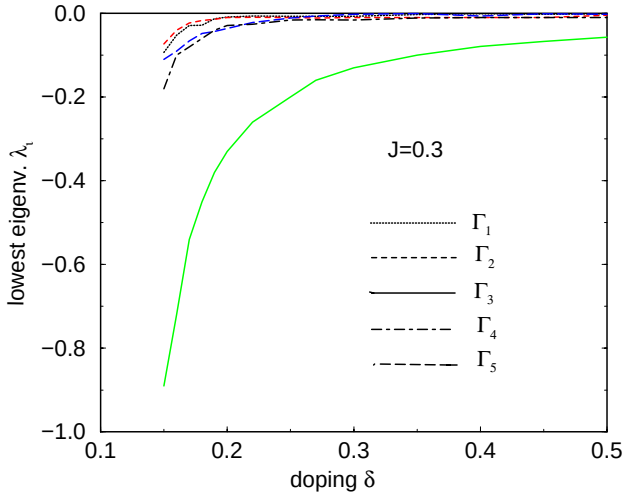

Fig. 2. Lowest eigenvalues λ_i of the static kernel Θ for the five representations Γ_i of C_{4v} as a function of the doping δ.

ω_c is a suitable cut-off and λ_i the smallest eigenvalue of a matrix which is essentially equal to the static limit of the kernel Θ and given by equation (10) of reference [11]. This matrix includes also the prefactor $1/N$ on the right-hand side of equation (40) and we put from now on N always equal to 2. Actually we will find that equation (62) is a rather poor approximation for T_c because Θ contains instantaneous and retarded contributions which have different cut-offs. Nevertheless the study of the static kernel Θ and its lowest eigenvalues has traditionally played a great role in discussing superconductivity in $t - J$ models.

Figure 1a shows the terms $\Theta^{(1)}$ and $\Theta^{(2)}$ and Figure 1b the terms $\Theta^{(3)}$,$\Theta^{(4)}$ and Θ for singlet pairing at zero frequencies for a fixed first momentum $\mathbf{k} = (2.465,0.309)$ as a function of the second argument $\mathbf{k}'$. $\mathbf{k}'$ moves counterclockwise around the Fermi line passing through the points $X, Y(\bar{X}, \bar{Y})$ along the positive (negative) x- and y-axis, respectively. Note that the letters X, Y denote not the $\mathbf{k}$-points $(\pi, 0), (0, \pi)$ but the points on the Fermi line between the Γ-point and the points $(\pi, 0), (0, \pi)$, respectively. The doping is $\delta = 0.17$ and $J = 0.3$. We used 22 $\mathbf{k}$-points along 1/8 of the Fermi line and a net of 300×300 $\mathbf{k}$-points in the Brillouin zone. Positive values of Θ mean repulsion, negative ones attraction between electrons in the s-wave channel. $\Theta^{(1)}$ and $\Theta^{(2)}$ originate from the normal, $\Theta^{(3)}$ and $\Theta^{(4)}$ from the anomalous vertex. $\Theta^{(1)}$ is due to instantaneous, the other terms due to retarded interactions. The figures show that $\Theta^{(4)}$ and $\Theta^{(1)}$ are by far the largest contributions. Both are dominated by the d-wave component and add up in a coherent way. $\Theta^{(4)}$ has different signs for singlet and triplet pairings. This as well as the explicit calculation shows that important contributions to $\Theta^{(4)}$ come from spin fluctuations within the partially filled band. There are no spin contributions related to the Heisenberg term and the magnon spectrum at zero doping because these terms are at least one order in $1/N$ smaller than the considered ones. $\Theta^{(3)}$ is due to charge (and spin) excitations and it is very small. Finally, $\Theta^{(2)}$ is due to charge fluctuations and consists of an attractive s-wave component (which, however, is cancelled by a repulsive s-wave term in $\Theta^{(1)}$) and a d-wave part which cancels partially that of the $\Theta^{(1)}$ term. Figure 1 demonstrates the importance of anomalous vertex contributions to Θ, the d-wave character of the leading contributions, and the competition between instantaneous and retarded interactions.

Figure 2 shows the lowest eigenvalues λ_i for each of the five representations Γ_i. In the calculation we used 5 $\mathbf{k}$-points along 1/8 of the Fermi line and a net of 300×300 $\mathbf{k}$-points in the Brillouin zone. The eigenvalues λ_i decrease with decreasing doping δ and diverge at $\delta \sim \delta_{BO} \sim 0.13$. At this doping value one of the six eigenvalues of the 6×6 matrix $1 + \chi$ in equation (45) goes through zero . As a result there is a soft mode which freezes into a static incommensurate bond-order wave of d-wave symmetry

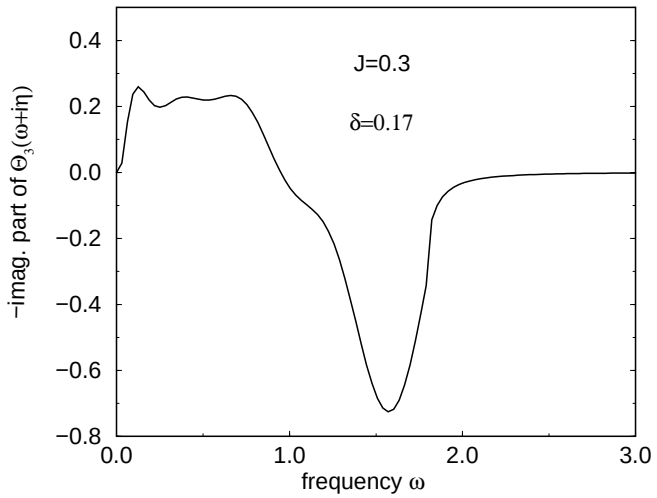

Fig. 3. Negative imaginary part of the d-wave projected kernel $\Theta_3(\omega + i\eta)$ as a function of the frequency ω using $\eta = 0.005$.

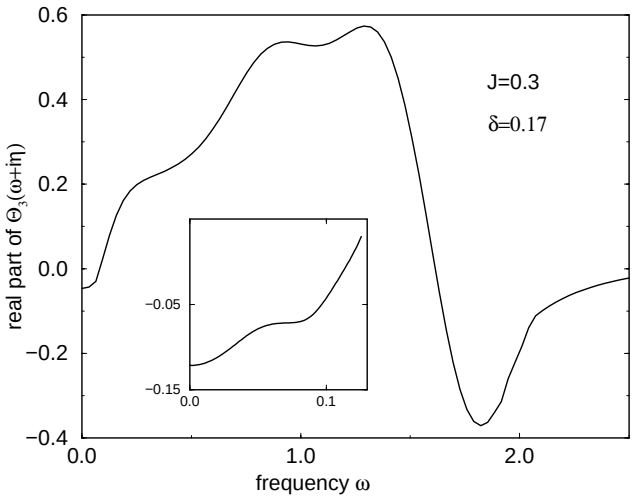

Fig. 4. Real part of the d-wave projected kernel $\Theta_3(\omega + i\eta)$ as a function of the frequency ω for $\eta = 0.005$. Inset: the same for small frequencies using $\eta = 0.002$.

for $\delta < \delta_{BO}$. This instability causes a divergence in some of the contributions to Θ at δ_{BO} and, as a precursor, the large negative values seen in Figure 2 for $\delta \leq 0.15$. The solid line in Figure 2 exhibits the lowest eigenvalue λ_3 associated with d-wave pairing. Its absolute magnitude is much larger than all the other eigenvalues and this is true for all dopings. Inserting λ_i into equation (40) it is clear that superconducting instabilities for non-d-wave symmetries are more of academic interest because the corresponding $T_c's$ would be extremely small. One concludes that the normal state is generally unstable against superconductivity in every symmetry channel but that only the d-wave (Γ_3) instability is strong enough to account for high transition temperatures.

4.2 Frequency dependence of Θ

For either even or odd frequency pairing the frequency dependence of Θ can be rewritten in terms of one frequency argument ω_n which is equal to the difference of the two original frequency variables. In order to illustrate the frequency dependence of the retarded part of Θ, Θ^{ret}, in the case of d-wave scattering, we average the momenta in Θ^{ret} over the Fermi line in the irreducible Brillouin zone using the eigenvector of the lowest eigenvalue λ_3. Finally we perform the analytic continuation $i\omega_n \to \omega + i\eta$.

Figure 3 shows the negative imaginary part of $\Theta_3^{ret}(\omega + i\eta)$ for $\eta = 0.005$. It is the analogue of the familiar function $\alpha^2 F(\omega)$ of Eliashberg theory for phonon-induced s-wave superconductivity. In our case this function is no longer positive-definite. This is a result of the projection of the total kernel on the Γ_3 symmetry. This projection involves a sum of $\mathbf{k}'$ over the 8 symmetry-related points along the Fermi line with factors determined by the representation i. In the case of d-wave pairing these factors are positive for small and large momentum transfers (of the order of a reciprocal lattice vector) and negative for intermediate momentum transfers of about half of a reciprocal lattice vector. For collective density fluctuations described by $\Theta^{(2)}$ this means that high-frequency contributions appear with a negative and low-frequency contributions with a positive sign in the d-wave kernel. A similar behavior is found for the other contributions. As a result $-\mathrm{Im}\Theta_3^{ret}$ is positive for $\omega \leq \omega_2 \sim |t|$ and negative for $\omega \geq \omega_2$. Using a momentum average with a constant weigth of Θ^{ret} corresponding to constant s-wave pairing would yield a curve which is similar to that in Figure 3 for $\omega \leq \omega_2$ but opposite in sign for $\omega \geq \omega_2$. $-\mathrm{Im}\Theta_3^{ret}$ describes the spectral distribution and spectral weight of spin and charge excitations involved in d-wave scattering. This function extends over a wide frequency region of about $2|t|$. Its high-frequency part is typical for collective charge fluctuations. It also contains substantial spectral weight at lower frequencies exhibiting a rather linear increase in frequency at the low-frequency end of the spectrum. Figure 4 shows the corresponding real part of Θ_3^{ret}. It is weakly negative at low frequencies up to about $\omega_1 \sim J/2$, changes then from negative to positive values until about $\omega \sim \omega_2$. The retarded interaction between electrons is thus attractive for $0 \leq \omega \leq \omega_1$ and strongly repulsive for $\omega_1 \leq \omega \leq \omega_2$. Somewhat above ω_2 the real part of Θ_3^{ret} jumps to large negative values and approaches zero from below in the high-frequency limit. The inset of Figure 4 shows the real part of Θ_3 at small frequencies with a larger resolution using $\eta = 0.002$.

4.3 Transition temperatures

Figures 1a and 1b show that the instantaneous and the retarded contributions to Θ are of similar magnitude and often compete with each other. In the calculation of T_c they are associated with quite different cut-offs. The instantaneous part is characterized by a cut-off determined by the width of the effective band whereas the cut-off relevant for the retarded part is set by the frequency range

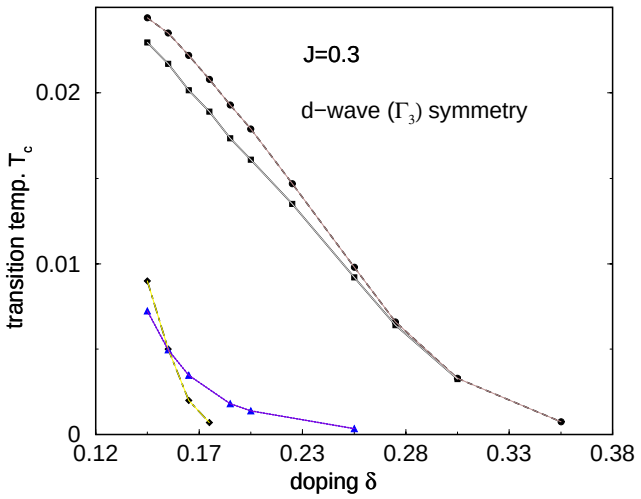

Fig. 5. Transition temperature T_c (with $|t|$ as energy unit) for Γ_3 pairing using the total kernel (squares), the instantaneous part (circles), the retarded part (diamonds) of the kernel, and the total kernel without charge-charge term (triangles).

where attraction dominates characterized roughly by J. In view of these complications we developed a method to solve equation (40) directly, avoiding the use of pseudopotentials. The only simplification we use is to put the momenta of the retarded kernel on the Fermi line. The validity of this approximation has been checked numerically and holds very well in our case. Using the fact that the instantaneous kernel consists only of a few separable contributions equation (40) can be reduced to a linear matrix problem. The number of rows and columns are given by the number of considered Matsubara frequencies times the number of **k**-points on the Fermi line in the irreducible Brillouin zone. Numerical tests showed that well converged results can be obtained with about 300 Matsubara frequencies and 5 **k**-points along 1/8 of the Fermi line down to values for T_c of ~ 0.002. Details of our method will be given elsewhere.

The squares in Figure 5 (joined by a solid line) show T_c for Γ_3-symmetry for doping $\delta > \delta_{BO}$. The broken line exhibits T_c if only the instantaneous part of the kernel is used. The dotted line corresponds to T_c if the charge-charge contribution (last term in Eq. (1)) is dropped. Finally the dashed-dotted line describes T_c if only the retarded kernel is taken into account.

In order to understand the curves in Figure 5 we consider the real part of the retarded kernel as a function of frequency, as shown in Figure 4. Taking only the part between zero and ω_2 into account would yield rather large values for T_c. To realize this one can decompose the real part into a large, constant repulsive part between $\omega = 0$ and $\omega = \omega_2$ plus the difference which is non-zero and attractive at low frequencies. Changing the cut-off from ω_2 to ω_1 using a pseudopotential description decreases strongly the effective repulsion yielding a large net attraction between 0 and ω_1 and thus a high value for T_c. Model calculation show that the large negative part in the real part of Θ_3 above ω_2 is very harmful to superconductivity: Lowering first the cut-off from $\sim 3|t|$ to ω_2 increases the effective potential, reducing further the cut-off to ω_1 decreases again the effective potential. The overall result is a rather modest attraction between $\omega = 0$ and $\omega = \omega_1$. This explains the rather low values for T_c calculated from the retarded part of Θ alone, as shown by the dash-dotted line in Figure 5. An alternative consideration would start from the instantaneous part in Θ leading to the transition temperatures shown by the broken line in Figure 5. Using a realistic value for the energy unit of about 8000 K (note that the usual effective hopping t_{exp} corresponds according to Eq. (1) to $|t|/2$) these values are already of the order of 100 K and comparable to the experimental ones. Adding the retarded part of the kernel does not lead to a further increase in T_c but rather to a slight decrease as illustrated by the squares in Figure 5. Model calculations show that a purely attractive Θ^{ret} would always increase T_c. The observed lowering of T_c must therefore be due to the repulsive part in Θ^{ret} above ω_1. This part plays a role because the T_c due to the instantaneous part alone is large enough to couple strongly the frequencies above and below ω_1 in the gap equation. The doping dependence of T_c is determined by various processes which compete with each other. For instance, the density of states decreases with doping which decreases the effective coupling. On the other hand, the energy scale for T_c is in the case of the instantaneous term set by the effective band width which increases with doping. Figure 5 shows that the net effect of these and other processes is to lower T_c substantially with increasing doping for $\delta > \delta_{BO}$. The eigenvalue λ_3 of the static kernel assumes according to Figure 2 large negative values near δ_{BO} anticipating the incipient bond-order wave instability. The associated soft mode does not affect the instantaneous but the retarded part. Figure 5 shows that the dashed line indeed increases steeply approaching δ_{BO} from above. On the other hand little effects are seen in the squares representing the full calculation. The reason for this is that at the low T_c's of the dashed curve the relevant frequencies lie in the attractive region of Θ_3^{ret} whereas for the high T_c values of the squares these frequencies lie already in the repulsive part. From this one may conclude that neither soft modes nor large negative eigenvalues of the static kernel guarantee large T_c values. In particular, there is no simple connection between T_c and λ_3.

The squares (connected by a dashed line) in Figure 6 show T_c as a function of the exchange constant J for a doping $\delta = 0.17$. T_c approaches 0 for $J \to 0$ in agreement with previous findings [11]. Except at small values of J T_c depends linearly on J. This is quite in contrast to the BCS-formula with an exponential dependence on J. The main reason for this is that the instantaneous term plays a major role and the momenta in it cannot confined to the Fermi surface in calculating T_c. Equation (53) is then a more appropriate formula for T_c. It is, however, too simple to argue that b_3 in that formula is rather independent on J and $\sim 1/T$ for $T \geq 0.01$. The rather perfect linear behavior is the result of more subtle dependencies such

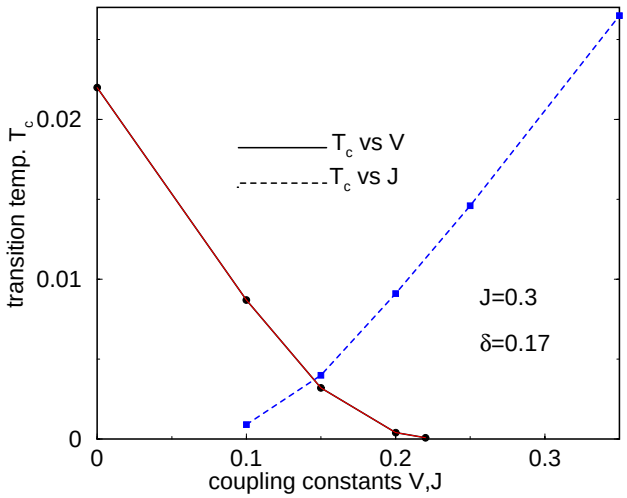

Fig. 6. Transition temperature T_c for Γ_3 pairing *versus* V (circles) and *versus* J (squares).

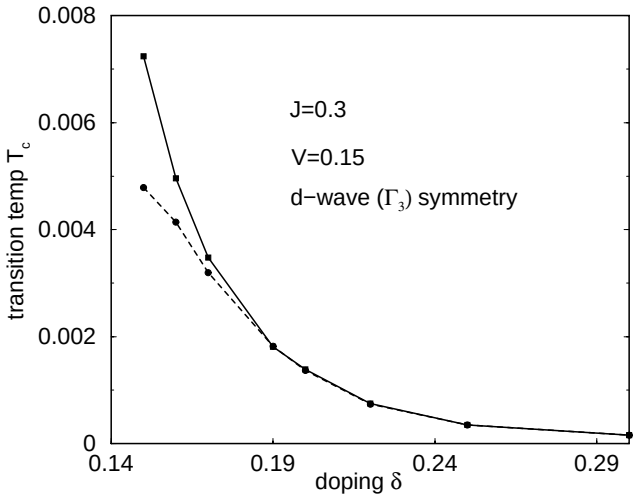

Fig. 7. Transition temperature T_c for Γ_3 pairing for $V = 0.15$ using the total kernel (squares) and the instantaneous part of the kernel (circles).

as the J-dependence of the one-particle energies and the non-rigidity of the bands as a function of J.

It has been argued [21,22] that the nearest-neighbor Coulomb potential V is not negligible in the cuprates. Adding this term

$$H' = \frac{V}{2N} \sum_{\substack{\langle ij \rangle \\ p,q=1\ldots N}} X_i^{pp} X_j^{qq}, \tag{63}$$

to the Hamiltonian equation (1) we have calculated T_c as a function of V. The circles (connected by a solid line) in Figure 6 present the result for $J = 0.3$ and $\delta = 0.17$. T_c decreases strongly with increasing V and is extremely small for $V \geq 3J/4$. This may be understood by looking just at the instantaneous term: equation (63) yields an additional term $2V(\mathbf{k} - \mathbf{k}')$ on the right-hand side of equation (43), canceling the J-terms exactly for $V = J$. T_c would thus vanish if only the instantaneous term would be present. For $V = J/2$ H' cancels the charge term in equation (1). According to Figure 6 this means a drop of T_c by about a factor 5 compared to the value at $V = 0$ which also agrees with Figure 5. Such a big drop of T_c due to the charge term of the $t-J$ model seems very surprising because the latter can only produce effects $\sim \delta^2$ and is therefore often omitted. Our calculation shows that this term cannot be neglected in a calculation of T_c and increases T_c substantially.

Figure 7 shows T_c as a function of δ for $J = 0.3$ and $V = 0.15$. Due to the Coulomb repulsion the T_c values are rather low. The important frequencies in the solution of the gap equation are also low and mainly located in the attractive region of the retarded kernel, Adding the retarded to the instantaneous part thus increases T_c. The two curves in Figure 7 demonstrate this effect.

Figures 8 and 9 show the influence of a second-nearest neighbor hopping term t' on T_c. In these figures a lower value of 0.2 has been chosen for J similar as in reference [9] in order to have a reasonably low δ_{BO} and a Van Hove

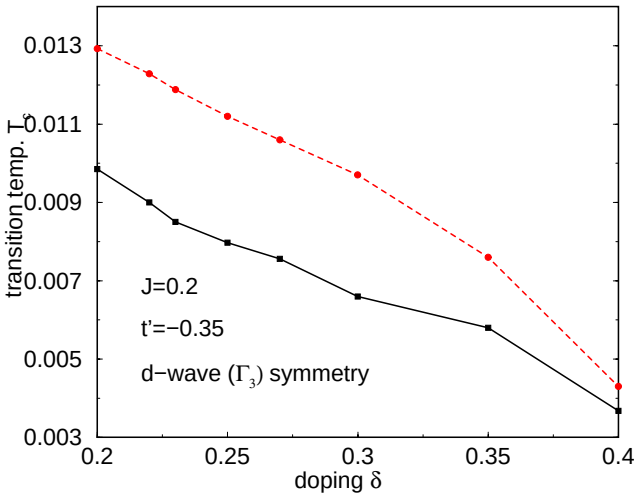

Fig. 8. Transition temperature T_c for Γ_3 pairing for $J = 0.2$ and $t' = -0.35$ using the total kernel (squares) and the instantaneous part of the kernel (circles).

singularity not too far away from optimal doping. Assuming a linear dependence of T_c on J the absolute values for T_c are similar in the corresponding Figures 5 and 8. T_c is thus rather robust to changes in t'. T_c decreases in Figure 8 somewhat slower than in Figure 5 due to the larger density of states in the surroundings of the Van Hove singularity. The difference between squares and circles is also larger in Figure 8 and decreases much slower with increasing doping. These effects are caused by the retarded part of the kernel which in Figure 8 is less attractive below ω_1 and more repulsive above ω_1 as shown in Figure 2 of reference [9] (note that the curve in that figure includes a constant instantaneous contribution of -0.29). The Van Hove singularity is located near $\delta = 0.28$. There is nearly no effect of the van Hove singularity on T_c for the same reasons as in the above case of the incipient bond-order

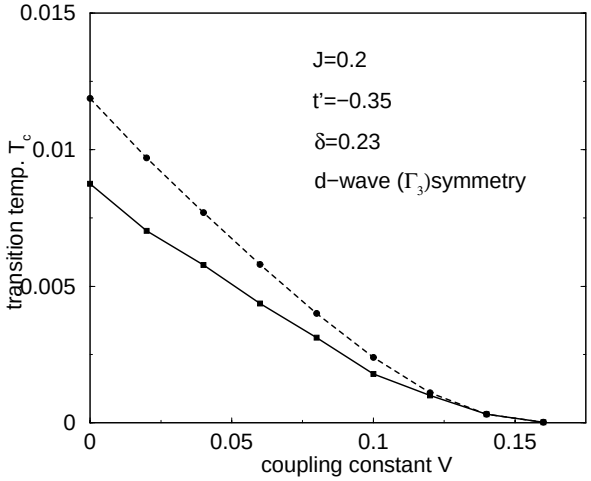

Fig. 9. Transition temperature T_c for $J = 0.2$, $t' = -0.35$, $\delta = 0.23$ as a function of V using the total kernel (squares) and the instantaneous part of the kernel (circles).

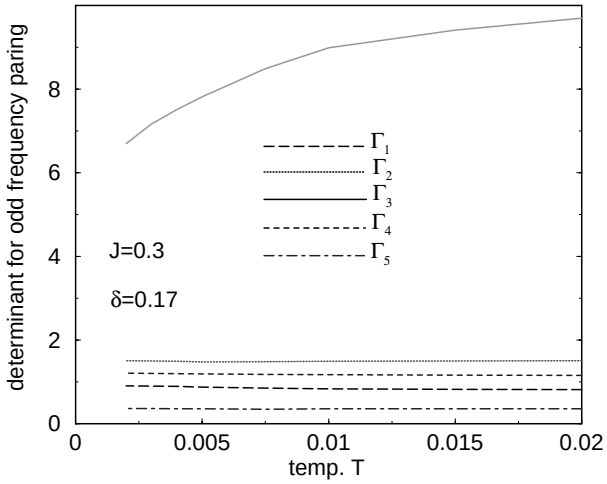

Fig. 10. Determinant associated with the gap equation for odd frequency pairing with symmetry Γ_i as a function of temperature T.

wave instability. (The curves in Fig. 3 of Ref. [9] were calculated without the charge-charge term and, erroneously, without the factor 1/2 in the instantaneous part. Correcting this error amounts essentially to lower the curves in that figure by about a factor 4.) Figure 9 should be compared with Figure 6. T_c decreases in both cases strongly with increasing V and practically vanishes for $V \geq J$.

We have also searched for superconducting instabilities with order parameters which are odd in frequency. The sum over Matsubara frequencies is always zero in this case so that the constraint of having no double occupancies of sites at the same time is automatically fulfilled for the two particles of the Cooper pair. There exists no static approximation for the kernel in this case. Possible instabilities are again determined by the linearized gap equation (40) where Σ_{an} and Θ have to be projected on the odd frequency parts. The transition temperature is determined by the condition that the determinant of a matrix consisting essentially of the kernel and the unity matrix is zero. In Figure 10 we have plotted this determinant as function of the temperature for each of the five irreducible representations using $J = 0.3$, $t' = 0.$, and $\delta = 0.17$. The Figure clearly shows that none of the curves tends to zero in the investigated temperature interval ruling out any odd frequency pairing instability with a T_c larger than ~ 0.002. This also can be seen directly from Figure 11 where the real part of $\Theta_3(\omega + i\eta)$ is shown for odd frequency pairing with Γ_3-symmetry corresponding also to triplet pairing. The effective interaction is repulsive up to energies $\sim t$ ruling out an instability towards superconductivity in this channel.

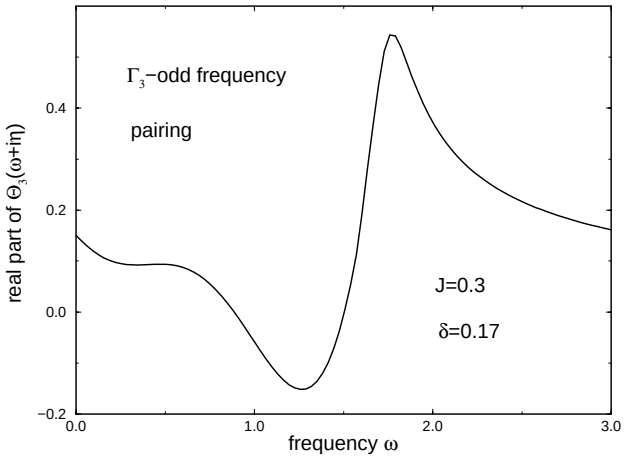

Fig. 11. Real part of the odd frequency, Γ_3 kernel $\Theta_3(\omega + i\eta)$ as a function of the frequency ω for $\eta = 0.005$.

4.4 Conclusions

Sections 2 and 3 demonstrate the feasibility of developing a perturbation expansion for the $t - J$ model in terms of X-operators and obtaining explicit expressions for the leading contributions to the anomalous self-energy of physical electrons using an $1/N$ expansion. The nonapplicability of Wick's theorem to X-operators does not cause any problem in such an approach. One also should note that the more involved and sophisticated parts of Sections 2 and 3 deal with contributions which are far beyond those considered in previous treatments. For instance, the slave boson $1/N$ result [3] for the anomalous self-energy corresponds in our approach just to the inhomogenous term in the integral equation (32). Similarly, only part of the first contribution to the kernel, $\Theta^{(1)}$, was calculated in reference [7] using a diagram technique for X-operators. This shows in our opinion that the employed functional approach is at least as suitable as other approaches to treat highly correlated Fermi systems. Taking also the numerical results of Section 3 into account our main conclusions

can be summarized as follows:

a) Our explicit expression for the $O(1/N)$ anomalous self-energy is clearly different from the corresponding expression of the slave boson theory. In particular, the largest contribution to the retarded kernel comes in the present approach from the anomalous part of the vertex and has no analogue in the slave boson approach. The presented expressions show for the first time in an explicit way that the $1/N$ expansions are really different in the two approaches. This difference can be traced back to different Hilbert spaces and different enforcement of the constraint. Even the order parameters for superconductivity are not related in a simple way: The leading slave boson order parameter involves necessarily (small) violations of local constraints in order to be nonzero whereas such violations are ruled out in our approach.

b) The kernel of the linearized gap equation consists of an instantaneous and an retarded part and both are similar in magnitude at low frequencies and for momenta near the Fermi surface. We found that there are superconducting instabilities in each symmetry channel and for all dopings. The true ground state thus never describes a Fermi liquid but a superconductor similar as in the weak coupling case [23]. However, these instabilities are in general extremely weak leading to academically low transition temperatures. The only clear and robust exception is the d-wavelike Γ_3 symmetry where a strong instability towards superconductivity occurs. Odd symmetry pairing mechanisms turned out to be very weak and can be ruled out as a mechanism for high-T_c superconductivity in our model.

c) In the case of Γ_3 symmetry the real part of the retarded kernel is weakly attractive at low frequencies on an energy scale of J or a fraction thereof and strongly repulsive at higher frequencies whereas the instantaneous part is attractive. Solving numerically the linearized gap equation the obtained transition temperatures T_c are for $N=2$ of the order of $0.01|t|$ and thus in principle large enough to account for the phenomena of high-T_c superconductivity. It is interesting to note that the Hubbard model at small or intermediate couplings also shows d-wave superconductivity with similar values for T_c [24]. The instantaneous term is instrumental in getting these large values for T_c: First, its cutoff is given by the effective band width and thus in general larger than J. Secondly, due to the large T_c, the solution of the gap equation involves large frequencies where the retarded term is strongly repulsive. As a result the retarded term is of less importance because attractive and repulsive parts of it cancel each other to a large extent. The dominance of the instantaneous part and the presence of two cutoffs lead to strong deviations from BCS-behavior. For instance, T_c depends linearly and not exponentially on J except at very small values for J.

d) T_c is rather insensitive to the addition of a second-nearest neighbor hopping term t' and to a Van Hove singularity. The latter can be understood by noting that the solution of the gap equation involves momentum and frequency averages in the instantaneous and retarded part, respectively, so that singularities in the density of states are washed out. T_c depends, however, sensitively on a nearest-neighbor Coulomb repulsion V and becomes very small if V is substantially larger than J.

e) Our calculations are limited to dopings larger than $\delta_{BO}(\sim 0.14$ for $J=0.3)$ where an instability towards an incommensurate bond-order wave of d-symmetry occurs. The associated soft mode causes $\lambda_3 \to -\infty$ for $\delta \to \delta_{BO}$ whereas T_c is nearly unaffected. In the underdoped regime $\delta < \delta_{BO}$ we expect a competition between bond-order and antiferromagnetic fluctuations which is beyond the leading order of the $1/N$ expansion considered in this investigation.

The second author (A. Greco) thanks the International Bureau of the Federal Ministry for Education , Science, Research and Technology for financial support (Scientific-technological cooperation between Argentina and Germany, Project n° ARG AD 3P) and the MPI-FKF for hospitality. Both authors acknowledge useful discussions with P. Horsch.

References

1. P.W. Anderson, *The Theory of Superconductivity in the High-T_c Cuprates* (Princeton University Press, Princeton, New Jersey, USA, 1997).
2. E. Dagotto, Rev. Mod. Phys. **66**, 763 (1994).
3. M. Grilli, G. Kotliar, Phys. Rev. Lett. **64**, 1170 (1990).
4. A. Houghton, A. Sudbo, Phys. Rev. B **38**, 7037 (1988).
5. E.S. Heeb, T.M. Rice, Europhys. Lett. **27**, 673 (1994).
6. E. Dagotto, A. Nazarenko, A. Moreo, Phys. Rev. Lett. **74**, 310 (1995).
7. F. Onufrieva, S. Petit, Y. Sidis, Phys. Rev. B **54**, 12464 (1996).
8. N.M. Plakida, V.S. Oudovenko, P. Horsch, A.I. Liechtenstein, Phys. Rev. B **55**, 1 (1997).
9. R. Zeyher, A. Greco, Z. Phys. B **104**, 737 (1997).
10. G. Kotliar, J. Liu, Phys. Rev. Lett. **61**, 1784 (1988).
11. A. Greco, R. Zeyher, Europhys. Lett. **35**, 115 (1996).
12. R. Zeyher, Molec. Phys. Rep. **17**, 247 (1997).
13. J.C. Guillou, E. Ragoucy, Phys. Rev. B **52**, 2403 (1995).
14. A.E. Ruckenstein, S. Schmitt-Rink, Phys. Rev. B **38**, 7188 (1988).
15. E. Abrahams, A. Balatsky, D.J. Scalapino, J.R. Schrieffer, Phys. Rev. B **52**, 1271 (1995).
16. G. Baym, L. Kadanoff, Phys. Rev. B **124**, 287 (1961).
17. R. Zeyher, M.L. Kulić, Phys. Rev. B **53**, 2850 (1996).
18. M.L. Kulić, R. Zeyher, Mod. Phys. Lett. B **11**, 333 (1997).
19. R. Zeyher, M.L. Kulić, Phys. Rev. B **54**, 8985 (1996).
20. I.S. Sandalov, M. Richter, Phys. Rev. B **50**, 12855 (1994).
21. L.F. Feiner, J.H. Jefferson, R. Raimondi, Phys. Rev. B **53**, 8751 (1996).
22. J. Riera, E. Dagotto, Phys. Rev. B **57**, 8609 (1998).
23. W. Kohn, J.M. Luttinger, Phys. Rev. Lett. **15**, 524 (1965).
24. D.J. Scalapino, Phys. Rep. **250**, 329 (1995).